

Two cobalt and nickel coordination polymers constructed from 1,4-bis(1,2,4-triazol-1-ylmethyl)benzene: Crystal structure and magnetic properties

Juanjuan Wang, Xiaoyan Xing, Yungai Li, Zan Sun, Qinglun Wang, Licun Li *

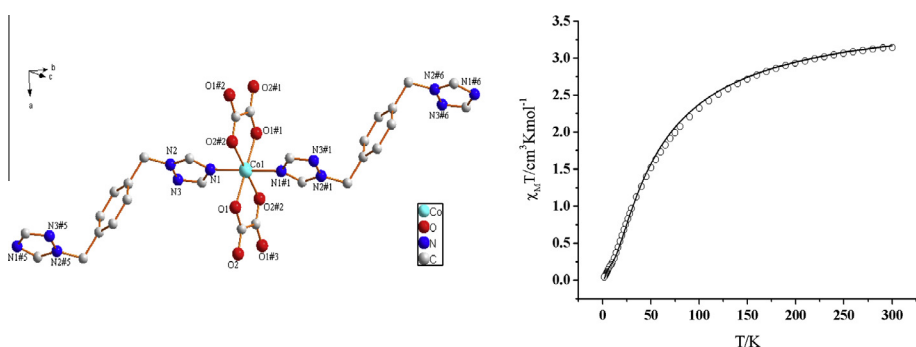
Department of Chemistry, Key Laboratory of Advanced Energy Materials Chemistry, Nankai University, Tianjin 300071, China
Tianjin Key Laboratory of Metal and Molecule-based Material Chemistry, Nankai University, Tianjin 300071, China



HIGHLIGHTS

- New transition metal coordination polymers with flexible bis(*N*-heterocycle) ligand.
- Both complexes show 2D network.
- The oxalate ligands mediate important antiferromagnetic coupling in cobalt complex.

GRAPHICAL ABSTRACT



ARTICLE INFO

Article history:

Received 13 March 2014

Received in revised form 10 April 2014

Accepted 10 April 2014

Available online 19 April 2014

Keywords:

Bis(triazole)

Transition metal

Coordination polymer

Magnetic properties

ABSTRACT

Two new transition metal coordination polymers with 1,4-bis(1,2,4-triazol-1-ylmethyl)-benzene(bttx), $[Ni(bttx)(ip)(H_2O)]$ (**1**) and $[Co(bttx)(ox)] \cdot 2H_2O$ (**2**) (H_2ip = isophthalic acid; ox = oxalate) have been synthesized and characterized. Single crystal X-ray diffraction analyses reveal compounds **1** and **2** are two-dimensional structure in which the flexible bis(triazole) ligands act as bridging ligands. The variable-temperature magnetic susceptibility data show that two compounds exhibit weak antiferromagnetic interactions. The magnetic behaviors are explained in connection with the crystal structure.

© 2014 Elsevier B.V. All rights reserved.

Introduction

Recently, coordination polymers have received considerable attention because of their variety of intriguing architectures and topologies as well as their potential applications in magnetism [1–3], luminescence [4,5], catalysis [6–8], and molecule storage [9–11]. As is known, the formation of coordination polymers is

highly sensitive to the character of organic ligands, the metal ions, pH value of the solution, the counterions, and the ratio between metal salt and ligands [12–21] and so on. Among these factors, the choice of the ligands is the key factor, which can influence the construction of coordination polymers with distinctive structures. It is well established that the *N*-containing ligands are regarded as the excellent candidates to construct coordination polymers [22–24]. The long flexible bis(*N*-heterocycle) organic ligands containing *N* donor atoms are especially attractive because *N*-heterocyclic units can bridge metal ions to produce polymers

* Corresponding author. Tel.: +86 22 23505465.

E-mail address: licun@nankai.edu.cn (L. Li).

with versatile structural motifs. Simultaneously, these flexible bis(*N*-heterocycle) ligands with their conformational freedoms increase the coordination versatility and provide additional spacing and the formation of stable open frameworks [25–28]. A number of coordination polymers based on the flexible bis(*N*-heterocycle) ligands have been reported [29–32]. For the flexible bis(*N*-heterocycle) ligands, 1,4-bis(1,2,4-triazol-1-ylmethyl)-benzene (btx) possesses the merits of triazole which can coordinate with the metal ions in various modes. In addition, the phenylene ring and triazole ring can freely rotate to meet the requirements of the coordination geometries of metal atoms on the basis of its –CH₂– spacer [33–35]. A few coordination polymers based on btx ligand has been reported, which exhibit the interesting structures and properties [36–42].

With this background information, we choose the bis(*N*-heterocycle) flexible ligand 1,4-bis(1,2,4-triazol-1-ylmethyl)benzene(btx) as bridging ligands in combination with isophthalic acid/oxalate to build new coordination polymers. Two new polymers, namely, [Ni(btx)(ip)(H₂O)] (**1**) and [Co(btx)(ox)]·2H₂O (**2**) (H₂ip = isophthalic acid; ox = oxalate) have been constructed successfully. Both two compounds exhibit two-dimensional layer structure. We report herein the synthesis, crystal structure, and magnetic properties of the two compounds. Magnetic data reveal weak antiferromagnetic coupling for compounds **1** and **2**.

Experimental

Materials and physical measurements

All commercially available reagents were used as received without further purification. The ligand 1,4-bis(1,2,4-triazol-1-ylmethyl)benzene was prepared according to the reported procedures [43]. Elemental analysis (EA) for C, H, and N was performed on a Perkin-Elmer 240 analyzer. Variable-temperature magnetic susceptibilities were measured on a SQUID MPMS XL-7 magnetometer. Diamagnetic corrections were made with Pascal's constants for all the constituent atoms.

Synthesis of complexes

Synthesis of [Ni(btx)(ip)(H₂O)] (**1**)

The mixture of NiCl₂·6H₂O (0.0475 g, 0.2 mmol), isophthalic acid (0.0332 g, 0.2 mmol), and btx (0.048 g, 0.2 mmol) was dissolved in 10 mL of distilled water. The pH value was then adjusted to 6.0 with 1 M NaOH solution. The resulting solution was transferred and sealed in a 25 mL Teflon-lined stainless steel vessel and heated at 160 °C for 2 days. The green crystals were obtained after the reaction system was slowly cooled to room temperature. The yield was 0.065 g (68%). Anal. Calcd. for C₂₀H₁₈N₆NiO₅ (%): C, 49.93; H, 3.77; N, 17.47. Found: C, 49.70; H, 3.88; N, 17.20. IR (KBr, cm^{−1}): 3413(m), 3120(w), 1607(m), 1525(s), 1479(w), 1440(w), 1404(m), 1372(s), 1283(w), 1134(m), 1022(w), 744(w), 721(m), 676(w).

Preparation of [Co(btx)(ox)]·2H₂O (**2**)

A mixture of CoCl₂·6H₂O (0.0476 g, 0.2 mmol), (NH₄)₂C₂O₄·H₂O (0.0284 g, 0.2 mmol), and btx (0.048 g, 0.2 mmol) was dissolved in 10 mL of distilled water and then was stirred in room temperature for 0.5 h. The resulting solution was sealed in a 25 mL Teflon-lined stainless steel vessel and heated at 160 °C for 2 days and then slowly cooled to room temperature. Orange-yellow crystals suitable for X-ray diffraction analysis were obtained when the reactor was cooled to room temperature from reaction temperature. The yield was 0.049 g (58%). Anal. Calcd. for C₁₄H₁₆CoN₆O₆ (%): C, 39.73; H, 3.81; N, 19.86. Found: C, 39.68; H, 3.76; N, 19.83. IR

Table 1
Crystal data and structure refinements for compounds **1** and **2**.

Empirical formula	C ₂₀ H ₁₈ N ₆ NiO ₅	C ₁₄ H ₁₆ CoN ₆ O ₆
Formula weight	481.09	423.26
Crystal system	Triclinic	Triclinic
space group	P̄I	P̄I
a(Å)	10.118(2)	5.4013(11)
b(Å)	10.399(2)	8.9450(18)
c(Å)	11.026(2)	9.6153(19)
α(°)	73.03(3)	75.25(3)
β(°)	68.12(3)	79.13 (3)
γ(°)	69.96(3)	85.84(3)
V(Å ³)	993.3(3)	441.04(15)
ρ _{calc} (mg/m ³)	1.615	1.594
F(000)	500	217
Crystal size (mm ³)	0.18 × 0.17 × 0.20	0.16 × 0.14 × 0.10
θ rang for data collection (°)	3.20–25.01	2.23–25.01
Limiting indices	−12 ≤ <i>h</i> ≤ −12; −12 ≤ <i>k</i> ≤ −12; −13 ≤ <i>l</i> ≤ −13	−6 ≤ <i>h</i> ≤ −5; −10 ≤ <i>k</i> ≤ −10; −11 ≤ <i>l</i> ≤ −10
Goodness-of-fit on F ²	1.056	1.070
R1, wR2 [<i>I</i> > 2σ (<i>I</i>)]	0.0369/0.0959	0.0572/0.1599
Max. difference peak, hole (eÅ ^{−3})	0.970, −0.533	0.667, −0.715

Table 2
Selected bond distances (Å) and angles (°) for compound **1**.

Ni(1)–O(4)#1	2.0021(19)	Ni(1)–N(1)	2.069(2)
Ni(1)–N(4)	2.050(2)	Ni(1)–O(2)	2.113(2)
Ni(1)–O(1)	2.058(2)	Ni(1)–O(3)	2.1424(18)
O(4)#1–Ni(1)–N(4)	90.27(9)	O(4)#1–Ni(1)–O(1)	96.54(8)
N(4)–Ni(1)–O(1)	85.85(9)	O(4)#1–Ni(1)–N(1)	91.36(9)
N(4)–Ni(1)–N(1)	177.38(9)	O(1)–Ni(1)–N(1)	91.92(9)
O(4)#1–Ni(1)–O(2)	101.40(8)	N(4)–Ni(1)–O(2)	91.09(9)
O(1)–Ni(1)–O(2)	161.82(8)	N(1)–Ni(1)–O(2)	90.60(9)
O(4)#1–Ni(1)–O(3)	162.99(8)	N(4)–Ni(1)–O(3)	89.33(8)
O(1)–Ni(1)–O(3)	100.39(8)	N(1)–Ni(1)–O(3)	89.72(9)
O(2)–Ni(1)–O(3)	61.61(7)	C(12)–N(1)–Ni(1)	128.3(2)
C(16)–N(1)–Ni(1)	128.3(2)	C(2)–N(4)–Ni(1)	132.72(19)
C(8)–N(4)–Ni(1)	123.09(18)	C(1)–O(2)–Ni(1)	90.25(15)
C(1)–O(3)–Ni(1)	88.55(14)	C(14)–O(4)–Ni(1)#4	125.6(2)

Symmetry transformations used to generate equivalent atoms: #1: *x* + 1, *y*, *z*; #4: *x* − 1, *y*, *z*.

Table 3
Selected bond distances (Å) and angles (°) for compound **2**.

Co(1)–O(1)#1	2.071(2)	Co(1)–O(2)#2	2.091(2)
Co(1)–N(1)#1	2.129(3)		
O(1)–Co(1)–O(2)#2	98.87(9)	O(2)#2–Co(1)–N(1)	88.14(11)
O(1)#1–Co(1)–O(2)#2	81.13(9)	O(2)#3–Co(1)–N(1)	91.86(11)
O(1)–Co(1)–O(2)#3	81.13(9)	O(1)–Co(1)–N(1)#1	91.65(11)
O(1)#1–Co(1)–O(2)#3	98.87(9)	O(1)–#1–Co(1)–N(1)#1	88.35(11)
O(1)–Co(1)–N(1)	88.35(11)	O(2)#2–Co(1)–N(1)#1	88.47(10)
O(1)#1–Co(1)–N(1)	91.65(11)	O(2)#3–Co(1)–N(1)#1	88.14(11)

Symmetry transformations used to generate equivalent atoms: #1: *−x*, *−y* + 1, *−z* + 2; #2: *x* − 1, *y*, *z*; #3: *−x* + 1, *−y* + 1, *−z* + 2.

(KBr, cm^{−1}): 3479(m), 3137(w), 1618(s), 1520(m), 1440(w), 1358(w), 1314(w), 1274(w), 1119(m), 1014(m), 992(w), 806(w), 735(w), 680(w), 491(w).

Crystal structure determination and refinement

The single crystal structure data for compounds **1** and **2** were collected on a Bruker SMART1000 CCD with graphite monochromatic Mo Kα radiation ($\lambda = 0.71073 \text{ \AA}$) at room temperature. The structures were solved by direct method with SHELXS-97 program

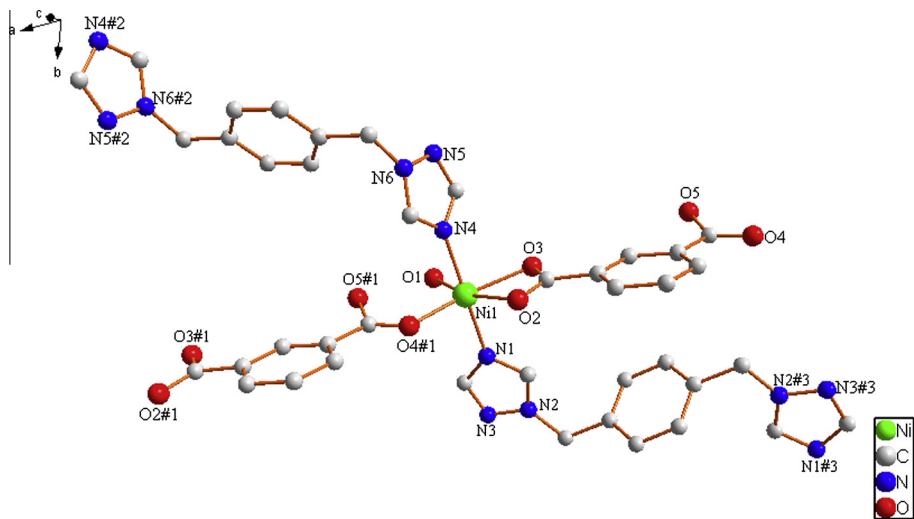


Fig. 1. The coordination environment of the Ni(II) ion in complex **1**. Symmetry codes: #1 $x + 1, y, z$; #2 $-x + 3, -y, -z + 2$; #3 $-x + 1, -y + 2, -z + 1$.

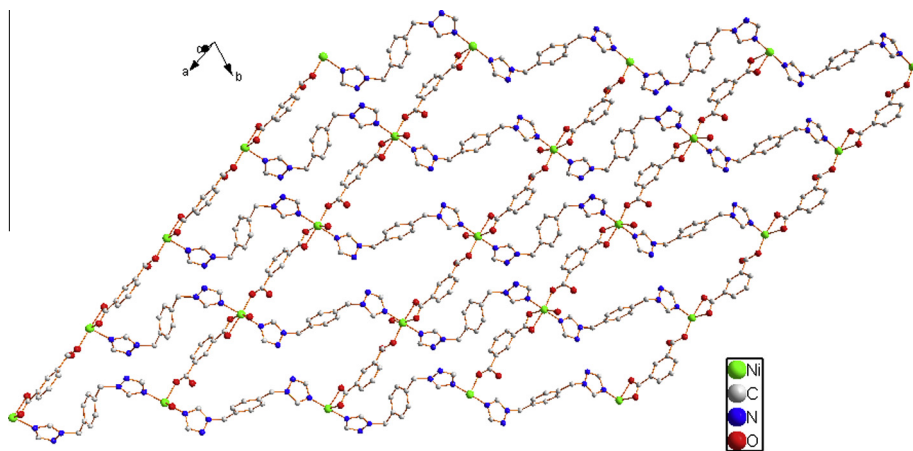


Fig. 2. The two-dimensional layer of $[\text{Ni}(\text{bttx})(\text{ip})(\text{H}_2\text{O})]$.

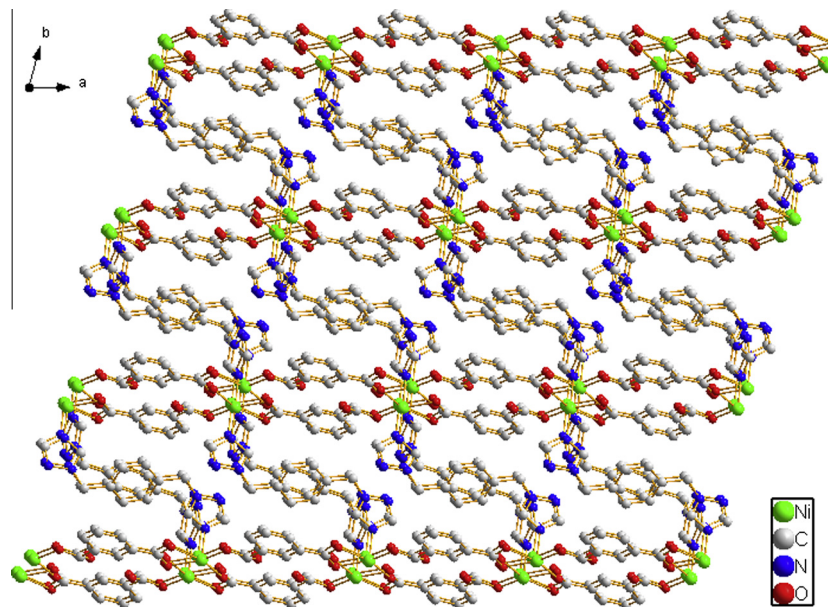


Fig. 3. A view of crystal packing of $[\text{Ni}(\text{bttx})(\text{ip})(\text{H}_2\text{O})]$ along c axis.

and refined by full-matrix least-squares on P^2 with SHELXL-97 program [44]. All non-hydrogen atoms were refined anisotropically, and hydrogen atoms were located and included at their calculated positions. The crystal data and structure refinement results are summarized in Table 1. Selected bond lengths and angles are listed in Table 2 and Table 3.

Results and discussion

Structure of $[Ni(btX)(ip)(H_2O)]$ (1)

X-ray single-crystal structure analysis reveals that **1** crystallizes in the triclinic space group $\bar{P}\bar{I}$. As shown in Fig. 1, each Ni(II) is six-coordinated in a distorted octahedral geometry by two nitrogen atoms ($N(1)$, $N(4)$) from two different btX ligands, two chelating carboxylate oxygen atoms ($O(2)$, $O(3)$) from the other ip²⁻, one carboxylate oxygen atom ($O(4)\#1$) from one ip²⁻ and one oxygen atom ($O(1)$) from the water molecule. The Ni-N bond distances are 2.068(2) Å and 2.050(2) Å for $Ni(1)-N(1)$ and $Ni(1)-N(4)$, respectively. The Ni-O bond lengths are in the range of 2.002–2.142 Å. Each ip²⁻ anion ligand acts as one μ_2 -bridge linking two nickel atoms, in which one carboxylate group adopts in $\eta^1:\eta^1$ coordination mode, while the other carboxylate group adopts in η^1 monodentate mode as depicted in Fig. 1. Each ip²⁻ anion through such coordinated modes connects adjacent Ni(II) atoms to yield 1D chain $[Ni(ip^{2-})_n]$ with Ni···Ni separation of 10.118(2) Å, and these 1D chains are further connected via *trans*-btX ligands to extend into a 2D motif containing square $Ni_4(btX)_2(ip^{2-})_2$ units

(Fig. 2). The Ni···Ni distances across the bridging btX are 12.677(5) Å and 14.028(6) Å, respectively. Within each layer, the basic grid of the two-dimensional network is puckered due to the conformation of the btX ligands, which results in two different sizes of $Ni_4(btX)_2(ip^{2-})_2$ units with large channels permitted by the 10.118(2) Å × 12.677(5) Å and 10.118(2) Å × 14.028(6) Å. A view of crystal packing of $[Ni(btX)(ip)(H_2O)]$ along the c axis is depicted in Fig. 3. There are two kinds of hydrogen bonding interactions originated the oxygen atom of the coordinated water molecule and the oxygen atoms from uncoordinated and chelated carboxyl group of ip²⁻. The oxygen atom from the coordinated water molecule acts as donor and the oxygen atoms from the carboxyl group act as acceptor. The hydrogen bonding distances of $O(1)-H(1B)\cdots O(5)\#1$ and $O(1)-H(1A)\cdots O(3)$ are 2.559(6) Å and 2.729(3) Å, of which the angle are 155° and 169°, respectively. These O-H···O hydrogen bonds of provides stability to the water molecules in this environment so that they can favors the stability of the sheet network.

Structure of $[Co(btX)(ox)] \cdot 2H_2O$ (2)

Compound **2** crystallizes in the triclinic space group $\bar{P}\bar{I}$. A view of the coordination sphere of the metal center is shown in Fig. 4. The Co(II) center is a inversion center and in a octahedral coordination sphere coordinated by four oxygen atoms ($O(1)$, $O(2)\#2$, $O(1)\#1$, $O(2)\#3$) from two oxalato-bridging ligands in the equatorial positions and two nitrogen atoms ($N(1)$, $N(1)\#1$) from two btX ligands as the apices. The bond distances of

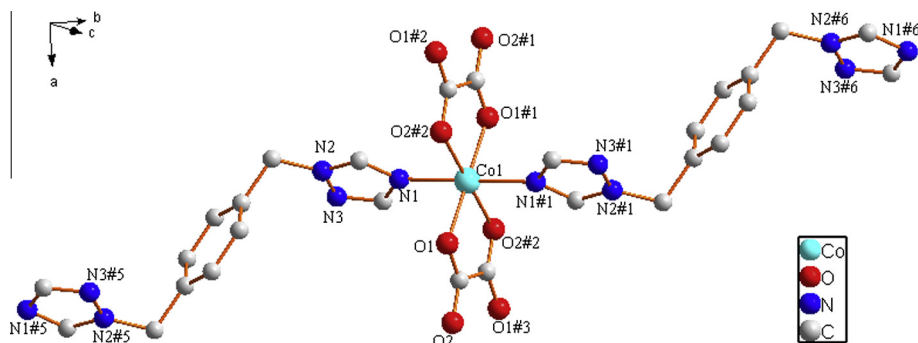


Fig. 4. The coordination environment of the Co(II) ion in complex **2**. symmetry codes: #1 $-x, -y + 1, -z + 2$; #2 $x - 1, y, z$; #3 $-x + 1, -y + 1, -z + 2$; #5 $-x + 1, -y, -z + 1$; #6 $1 + x, 1 + y, 1 + z$.

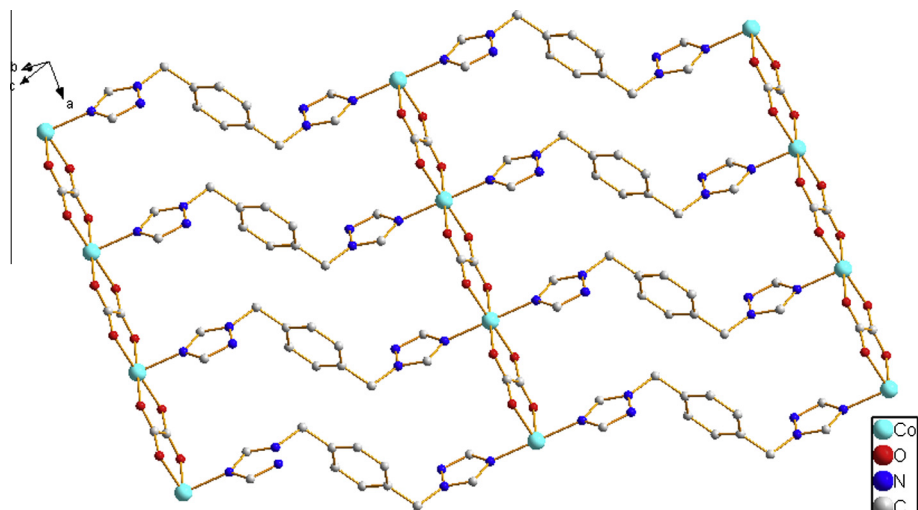


Fig. 5. The two-dimensional layer of $[Co(btX)(ox)] \cdot 2H_2O$.

Co1-O2#2 and Co(1)-O(1) are 2.091(2) Å and 2.071(2) Å, which are smaller than Co-N bond distance(2.135(3) Å). These bond distances are consistent with the reported Co(II) complexes [45]. The Co(II) centers are connected together by oxalates to form an linear chain $[Co(ox)]_n$, wherein the intrachain adjacent Co···Co separation is 5.401(1) Å. And in this way, such chains are further bridged through *trans*-btx ligands to give rise to two-dimension framework containing square $Co_4(bt_x)_2(ox)_2$ with channels of 5.401(1) Å × 14.793(4) Å (Fig. 5). A view of crystal packing of compound 2 along the *b* axis is depicted in Fig. 6.

Magnetic properties

The temperature dependence of the molar magnetic susceptibilities of compounds **1** and **2** were measured in 2–300 K range under an applied 2kOe dc field. The plots of $\chi_M T$ vs. T of the two compounds **1** and **2** are provided in Fig. 7 and Fig. 8, respectively.

For compound **1**, The $\chi_M T$ value at room temperature is $1.24 \text{ cm}^3 \text{ K mol}^{-1}$, which is slightly higher than expected for the spin-only value for a Ni(II) center ($\chi_M T = 1.00 \text{ cm}^3 \text{ K mol}^{-1}$ for $S = 1$). Upon cooling, $\chi_M T$ remains roughly constant until 50 K, then sharply decreases to $0.50 \text{ cm}^3 \text{ K mol}^{-1}$ at 2.0 K. Based on the structure, two exchange pathways can be considered: one is through ip^{2-} ligand; the other is through the btx ligands. However, the magnetic interactions through these exchange pathways should

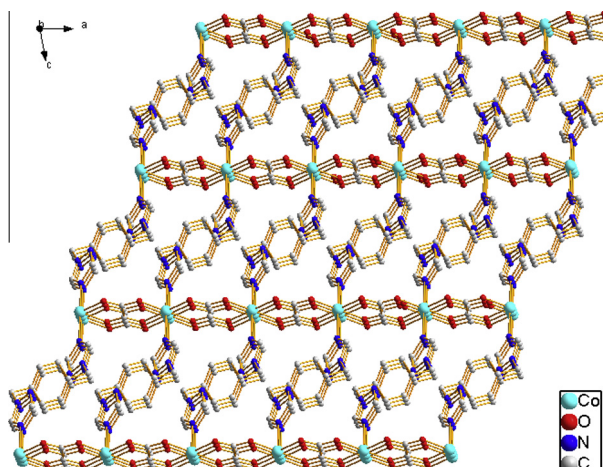


Fig. 6. A view of crystal packing of $[Co(bt_x)(ox)] \cdot 2H_2O$ along *b* axis.

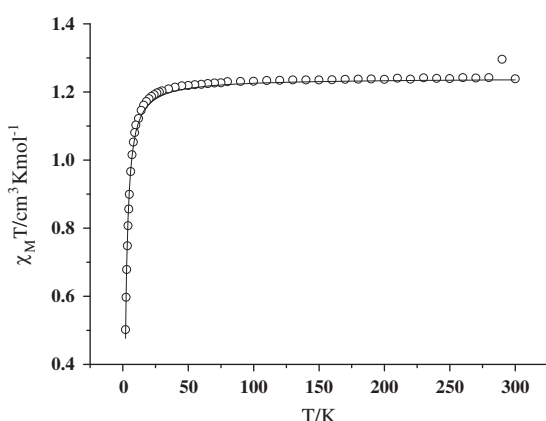


Fig. 7. Temperature dependence of the $\chi_M T$ product of compound **1**. The solid line corresponds to the theoretical best-fit.

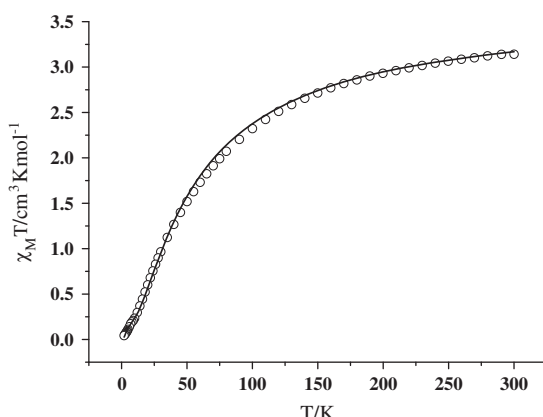


Fig. 8. Temperature dependence of the $\chi_M T$ product of compound **2**. The solid line corresponds to the theoretical best-fit.

be weak. As well known, the octahedral Ni (II) ion has important zero-field splitting. Thus, the experimental susceptibility data of **1** were fitted by using the following expressions when considered $S = 1$ ions in the presence of a single ion anisotropy and possible weak magnetic coupling (θ) between Ni(II) ions.

$$\chi_M = \frac{2Ng^2\beta^2}{3k(T-\theta)} \frac{2x^{-1} - 2\exp(-x)x^{-1} + \exp(-x)}{1 + 2\exp(-x)} \quad (1)$$

where $x = D/kT$. The best parameters fitted in the whole temperature range are $g = 2.23$, $D = 4.22 \text{ cm}^{-1}$, $\theta = -1.21 \text{ K}$ and $R = 5.98 \times 10^{-4}$ (R value is defined as $\Sigma[(\chi_M)_{\text{obs}} - (\chi_M)_{\text{calc}}]^2 / \Sigma[(\chi_M)_{\text{obs}}]^2$). The negative θ value suggests the weak antiferromagnetic interactions between the Ni^{II} ions.

For compound **2**, the $\chi_M T$ value at room temperature is $3.14 \text{ cm}^3 \text{ K mol}^{-1}$, which is higher than expected for the uncoupling value for a high-spin Co(II) center ($\chi_M T = 1.87 \text{ cm}^3 \text{ K mol}^{-1}$) due to orbital angular momentum. Upon cooling, $\chi_M T$ decreases continuously to reach $0.043 \text{ cm}^3 \text{ K mol}^{-1}$ at 2.0 K. The decreasing trend of $\chi_M T$ value with the temperature suggests the presence of antiferromagnetic interactions. The magnetic exchange coupling mediating by btx ligands are anticipated to be weak. Thus, from the viewpoint of magnetism, compound **2** can be treated as oxalate bridged one-dimensional Co(II) chain. Hence, comparing to reported one-dimensional Co(II) chain [46,47], although the magnetic measurements clearly indicate that the metal centers have a similar connectivity, it is insensitive to the different dimensionality of the two networks caused by the change in different conformation the ligand or adding other bridging ligand.

Recently, Rueff et al. have proposed a phenomenological approach for one-dimensional Co(II) systems that allows one to have an estimate of the strength of the antiferromagnetic exchange interactions by means of the expression (2): [48,49]

$$\chi_M T = A \exp(-E_1/kT) + B \exp(-E_2/kT) \quad (2)$$

in which $A + B$ equals the Curie constant and E_1 and E_2 represent the “activation energies” corresponding to spin-orbit coupling and the antiferromagnetic exchange interaction. The optimum magnetic parameters fitted in the whole temperature range are $E_1/k = 48.47 \text{ K}$, $E_2/k = 5.15 \text{ K}$, $A + B = 3.67 \text{ cm}^3 \text{ K mol}^{-1}$, $R = 4.75 \times 10^{-3}$. The fitting results show the magnetic coupling between Co(II) ions through oxalate is antiferromagnetic. According to the relationship of $\chi_M T \propto \exp(J/2kT)$, the obtained magnitude of exchange coupling is -7.15 cm^{-1} , which is comparable to those of the reported oxalate-bridged Co(II) complexes in literature and well confirms the antiferromagnetic interactions [50–52].

Conclusion

In summary, two transition metal compounds based on 1,4-bis(1,2,4-triazol-1-ylmethyl)benzene ligand have been successfully synthesized and characterized structurally and magnetically. The crystal structural analyses indicate that the two compounds have 2D layer structure. The magnetic studies show that magnetic behavior of compound **1** is dominated by the zero-field splitting (ZFS) of the Ni(II) ions, while there exists important antiferromagnetic coupling in compound **2** transmitted by oxalate ligands. This work has shown that the use of the flexible bis(*N*-heterocycle) organic ligand in combination with the dicarboxylate ligands is an efficient way for constructing interesting polymeric architectures with transition metal ions. It is believed that the simultaneous use of the flexible bis(*N*-heterocycle) organic ligand and the carboxylate ligands may provide a promising pathway to rational design of diversely connected metal–organic frameworks [25,27,28,30,34,37].

Acknowledgments

This work was supported by the National Natural Science Foundation of China (Nos. 91122013, 20971072, and 90922032), the NSF of Tianjin (No. 11JCYBJC03500) and MOE Innovation Team (IRT13022) of China.

Appendix A. Supplementary material

Supplementary data associated with this article can be found, in the online version, at <http://dx.doi.org/10.1016/j.molstruc.2014.04.038>.

References

- [1] M. Kurmoo, Chem. Soc. Rev. 38 (2009) 1353–1379.
- [2] H.B. Xu, B.W. Wang, F. Pan, Z.M. Wang, S. Gao, Angew. Chem., Int. Ed. 46 (2007) 7388–7392.
- [3] K.S. Gavrilenko, S.V. Punin, O. Cador, S. Golhen, L. Ouahab, V.V. Pavlishchuk, J. Am. Chem. Soc. 127 (2005) 12246–12253.
- [4] B. Zhao, X.Y. Chen, P. Cheng, D.Z. Liao, S.P. Yan, Z.H. Jiang, J. Am. Chem. Soc. 126 (2004) 15394–15395.
- [5] M.D. Allendorf, C.A. Bauer, R.K. Bhakta, R.J.T. Houk, Chem. Soc. Rev. 38 (2009) 1330–1352.
- [6] J. Lee, O.K. Farha, J. Roberts, K.A. Scheidt, S.T. Nguyen, J.T. Hupp, Chem. Soc. Rev. 38 (2009) 1450–1459.
- [7] L.Q. Ma, C. Abney, W.B. Lin, Chem. Soc. Rev. 38 (2009) 1248–1256.
- [8] Z.J. Zhang, L.P. Zhang, L. Wojtas, M. Eddaoudi, M.J. Zaworotko, J. Am. Chem. Soc. 134 (2012) 928–933.
- [9] J.R. Li, R.J. Kuppler, H.C. Zhou, Chem. Soc. Rev. 38 (2009) 1477–1504.
- [10] P.K. Thallapally, J. Tian, M.R. Kishan, C.A. Fernandez, S.J. Dalgarno, P.B. McGrail, J.E. Warren, J.L. Atwood, J. Am. Chem. Soc. 130 (2008) 16842–16843.
- [11] Y.B. Zhang, W.X. Zhang, F.Y. Feng, J.P. Zhang, X.M. Chen, Angew. Chem., Int. Ed. 48 (2009) 5287–5290.
- [12] X.Q. Lv, J.J. Jiang, H.C. zur Loye, B.S. Kang, C.Y. Su, Inorg. Chem. 44 (2005) 1810–1813.
- [13] Y.C. Gao, Q.H. Liu, F.W. Zhang, G. Li, W.Y. Wang, H.J. Lu, Polyhedron 30 (2011) 1–8.
- [14] L.S. Long, CrystEngComm 12 (2010) 1354–1365.
- [15] W.X. Ni, M. Li, X.P. Zhou, Z. Li, X.C. Huang, D. Li, Chem. Commun. (2007) 3479–3481.
- [16] C. Náther, G. Bhosekar, I. Jess, Inorg. Chem. 46 (2007) 8079–8087.
- [17] M.S. Chen, M. Chen, T.A. Okamura, W.Y. Sun, N. Ueyama, Microp. Mesop. Mater. 139 (2011) 25–30.
- [18] Z. Su, J. Fan, T. Okamura, W.Y. Sun, N. Ueyama, Cryst. Growth Des. 10 (2010) 3515–3521.
- [19] Y. Cheng, P. Xu, Y.B. Ding, Y.G. Yin, CrystEngComm 13 (2011) 2644–2648.
- [20] P. Mahata, A. Sundaresan, S. Natarajan, Chem. Commun. (2007) 4471–4473.
- [21] O. Fabelo, J. Pasán, L. Cañadillas-Delgado, F.S. Delgado, F. Lloret, M. Julve, C. Ruiz-Pérez, Inorg. Chem. 47 (2008) 8053–8061.
- [22] Y.F. Qi, K. Xu, L.J. Lu, J. Li, E.B. Wang, J. Coor. Chem. 66 (2013) 1228–1237.
- [23] M. Chen, Y. Lu, J. Fan, G.C. Lv, Y. Zhao, Y. Zhang, W.Y. Sun, CrystEngComm 14 (2012) 2015–2023.
- [24] U. García-Couceiro, O. Castillo, J. Cepeda, M. Lanchas, A. Luque, S. Pérez-Yáñez, P. Román, D. Vallejo-Sánchez, Inorg. Chem. 49 (2010) 11346–11361.
- [25] J.K. Sun, Q.X. Yao, Y.Y. Tian, L. Wu, G.S. Zhu, R.P. Chen, J. Zhang, Chem. Eur. J. 18 (2012) 1924–1931.
- [26] Z.G. Gu, X.X. Xu, W. Zhou, C.Y. Pang, F.F. Bao, Z.J. Li, Chem. Commun. 48 (2012) 3212–3214.
- [27] J. Zhao, D.S. Li, X.J. Ke, B. Liu, K. Zou, H.M. Hu, Dalton Trans. 41 (2012) 2560–2563.
- [28] L.Y. Xin, G.Z. Liu, X.L. Li, L.Y. Wang, Cryst. Growth Des. 12 (2012) 147–157.
- [29] G. Aromi, L.A. Barrios, O. Roubeau, P. Gamez, Coor. Chem. Rev. 255 (2011) 485–546.
- [30] M. Li, Q. Ling, Z. Yang, B.L. Li, H.Y. Li, CrystEngComm 15 (2013) 3630–3639.
- [31] S.L. Huang, H.W. Hou, L.W. Mi, Y.T. Fan, J. Coor. Chem. 62 (2009) 1964–1971.
- [32] N. Wang, Y.C. Feng, W. Shi, B. Zhao, P. Cheng, D.Z. Liao, S.P. Yan, CrystEngComm 14 (2012) 2769–2778.
- [33] Y.F. Peng, H.Y. Ge, B.Z. Li, B.L. Li, Y. Zhang, Cryst. Growth Des. 6 (2006) 994–998.
- [34] J. Yu, R. Yao, L. Yuan, B. Xu, B. Qu, W. Liu, Inorg. Chim. Acta. 376 (2011) 222–229.
- [35] J. Wang, J.Q. Tao, X.J. Xu, C.Y. Tan, Bull. Korean Chem. Soc. 33 (2012) 3827–3830.
- [36] L. Liu, B. Han, X.Q. Liang, Z. Yang, J.T. Jia, F.X. Sun, G.S. Zhu, J. Mol. Struct. 1047 (2013) 338–343.
- [37] Y. Deng, C.T. Hou, R.I. Walton, J.Q. Tang, P.Z. Zhu, K.L. Zhang, S.W. Ngc, Dalton Trans. 42 (2013) 12468–12480.
- [38] Y.T. Gou, F. Yue, H.M. Chen, G. Liu, D.C. Sun, J. Coor. Chem. 66 (2013) 1889–1896.
- [39] X. Zhu, P.P. Sun, J.G. Ding, B.L. Li, H.Y. Li, Cryst. Growth Des. 12 (2012) 3992–3997.
- [40] Z. Zhang, D.F. Wu, K. Hu, Y.J. Shi, Z.L. Chen, F.P. Liang, J. Coor. Chem. 66 (2013) 2499–2515.
- [41] X.Y. Xing, X.Y. Song a, P.P. Yang a, R.N. Liu, L.C. Li, D.Z. Liao, J. Mole. Struct. 967 (2010) 196–200.
- [42] H.Y. Ge, Y. Yang, Y.F. Peng, B.L. Li, Y. Zhang, J. Coor. Chem. 65 (2012) 3372–3382.
- [43] X.R. Meng, Y.L. Song, H.W. Hou, H.Y. Han, B. Xiao, Y.T. Fan, Y. Zhu, Inorg. Chem. 43 (2004) 3528–3536.
- [44] G.M. Sheldrick, Acta Crystallogr. A64 (2008) 112–122.
- [45] S.L. Huang, X.X. Li, X.J. Shi, H.W. Hou, Y.T. Fan, J. Mater. Chem. 20 (2010) 5695–5699.
- [46] E. Coronado, M. Giménez-Marqués, G.M. Espallargas, Inorg. Chem. 51 (2012) 4403–4410.
- [47] S.Y. Zhang, W. Shi, Y.H. Lan, N. Xu, X.Q. Zhao, A.K. Powell, B. Zhao, P. Cheng, D.Z. Liao, S.P. Yan, Chem. Commun. 47 (2011) 2859–2861.
- [48] D.H. Choi, J.H. Yoon, J.H. Lim, Inorg. Chem. 45 (2006) 5947–5952.
- [49] A. Majumder, V. Gramlich, G.M. Rosair, Cryst. Growth Des. 6 (2006) 2355–2368.
- [50] U. García-Couceiro, O. Castillo, A. Luque, J.P. García-Terán, G. Beobide, P. Román, Cryst. Growth Des. 6 (2006) 1839–1847.
- [51] S.C. Manna, E. Zangrandino, J. Ribas, N.R. Chaudhuri, Dalton Trans. (2007) 1383–1391.
- [52] U. García-Couceiro, O. Castillo, A. Luque, G. Beobide, P. Román, Inorg. Chim. Acta. 357 (2004) 339–344.